UILU-ENG 84-3612

Report No. 112

FATIGUE CRACK GROWTH IN GRAY CAST IRON UNDER STEP LOADING HISTORIES

by

Gary B. Marquis
Department of Mechanical and Industrial Engineering

A Report of the

MATERIALS ENGINEERING - MECHANICAL BEHAVIOR

College of Engineering, University of Illinois at Urbana-Champaign

October 1984

ACKNOWLEDGEMENTS

I would like to thank Professor F.A.Leckie for his supervision and helpful suggestions in completing this research.

Thanks is also due to J.L.Koch for his friendship and technical help throughout the project.

This investigation was conducted in the Materials Engineering Research Laboratory at the University of Illinois at Urbana under a grant from the National Science Foundation NSF-MEA-82-19593. The material tested was provided by John Deere and Company.

TABLE OF CONTENTS

I. INTRODUCTION

In the last 20 years, much research has been devoted to the study of wrought metal components under service loading situations. Relatively little work has been done to understand the fatigue processes present in ferrous-based cast materials. Methods developed to predict the fatigue response of wrought materials are often misapplied to cast materials. For example, mean stress parameters based on the reduction of static or fatigue properties are not appropriate for gray cast iron [1]. It is the intent of this research to help improve the understanding of basic fatigue mechanisms occuring in cast irons and to help in developing some simple analytical tools to analyze the fatigue resistance of cast iron components.

In wrought materials, a significant portion of the fatigue life of a specimen may be spent in the initiation of cracks. The number of cycles to initiate a crack is often added to the number of cycles required to propagate the crack to a critical size to give the total fatigue life of a component [2]. In cast iron, fatigue cracks initiate very early in the life of a specimen and then grow through a complex process of linking many graphite flakes and the linking of many crack systems. Because of the complexity of the crack growth process, simple crack growth equations, such as the Paris law, are not directly applicable to cast iron. Detailed studies of the initiation and growth of fatigue cracks have been made for both gray and nodular irons under constant amplitude stress or strain testing [3,4].

The fatigue resistance of cast iron has been shown to be highly dependent on the morphology of the graphite phase and the strength of the steel matrix material [5]. The graphite phase acts as sites of internal discontinuities and stress concentration. The graphite phase in gray cast iron exists in the form of sharp edged flakes. The flake edges provide regions of high stress concentration, so the matrix material near the flake will begin to yield even if the nominal tensile stress on a specimen is low. In compression, however, the flakes close up and support load. For these reasons, gray iron exhibits different monotonic behavior in tension and compression and asymmetric hysteresis loops during fatigue cycling. The graphite phase in nodular iron is nearly spherical. Because a sphere has a less severe stress concentration than does a flake, nodular iron has a higher tensile yield strength and better fatigue properties than does gray iron. Even with these limitations, because of its relatively low cost, excellent casting properties and good machinability, gray cast iron is still widely used in mechanical design.

Crack growth in gray cast iron under simple variable amplitude load histories and the effects of load sequence on crack growth rate have been studied. Polished cylindrical gray cast iron specimens were subject to Lo-Hi or Hi-Lo strain histories. Fatigue crack lengths were measured from surface replicas taken throughout the life of the specimens. Crack growth rates from these histories were compared to constant amplitude test data to evaluate the use of crack length data as a single state measure of fatigue damage. A multi-parameter continuum damage model has been proposed by Socie, Fash and Leckie to predict the fatigue life of irons under variable loading histories [6]. This model assumes that equivalent crack lengths represent equivalent states of fatigue damage. While this model seems to work better than Miner's rule in predicting the fatigue life of cast iron specimens subject to variable strain histories, it fails to predict some of the load sequence effects observed in this research program.

II. MATERIAL AND SPECIMEN PREPARATION

Test bars, 36mm in diameter and 200mm long, were cast in green sand molds to produce the pearlitic gray iron. Test specimens were machined from the as-cast bars to the dimensions given in Figure 1. The gage section of each specimen was finished using emery paper. The direction of finishing was alternated between axial and circumferential for the successively finer grades of emery paper. Final polishing was accomplished by rotating the specimen on a lathe while polishing with a felt pad mounted on a pneumatic rotary polishing rod. The felt pad was saturated with a solution of 0.3 micron alumina powder in water. The final polishing produced a mirror-like surface which provided good resolution of the surface replicas taken during testing.

Matrix microstructure and graphite flake structure, classified by ASTM A247 [7] as 60% type A, 40% type D, size 4, are shown in Figure 2. The average eutectic cell size was 0.14mm. Material chemistry is given in Table 1 and mechanical properties are given in Table 2. The monotonic stress-strain response is shown in Figure 3.

III. TESTING PROGRAM

Strain controlled material tests were performed on a servo-hydraulic test frame. All tests were digitally controlled and test data was collected, digitized and stored using a dedicated Intel 8840 single board computer. Upon completion of each test, data was stored on floppy disk or magnetic tape. An axial extensometer was used to monitor the material strain response and provide control feedback. Stress-strain hysteresis loops were recorded at every power of two cycles.

CONSTANT AMPLITUDE FATIGUE TESTS

Constant amplitude, uniaxial, totally reversed, strain controlled fatigue tests were performed on the cast iron specimens. At least two specimens were tested at each of three strain amplitudes: 0.002, 0.0015, and 0.001. Fatigue failure was defined as a 90% tensile load drop from the initial maximum tensile load. Tensile load data was taken on every power of two cycles and on cycles for which the peak tensile load decreased by a multiple of 5% from the peak tensile load recorded at the initiation of cycling.

VARIABLE AMPLITUDE FATIGUE TESTS

Test specimens were cycled at constant amplitude strain control until an estimated 30-70% of the fatigue life had been exhausted. The percentage fatigue life exhausted was estimated from the number of cycles completed, tensile load drop data, and failure crack length. The strain amplitude was then changed and fatigue cycling continued until failure. Each block of fatigue cycling was begun with a tensile peak and completed after a compressive peak. After the compressive reversal the strain was returned to zero before the next block of cycling was begun. Because of the hysteresis response of the material, a slight tensile load was required to return the strain to zero. This tensile load had some effect on the mean stress; in the worst situation ($\Delta\epsilon_1/2$=.002, $\Delta\epsilon_2/2$=.001) the mean stress was increased by about 7 MPa compared to a total stress range at $\Delta\epsilon_1/2$=.001 of 196 MPa. All tests were run with zero mean strain. Using this procedure, three different Lo-Hi and three Hi-Lo strain histories were tested. The initial and final strain amplitudes in each history were equivalent to one of the three strain amplitudes previously tested during the constant amplitude fatigue cycling. Strain histories are shown in Figure 4. Two samples were tested at each of the six different strain histories.

SURFACE CRACK GROWTH

Surface crack initiation and growth were monitored during both the constant amplitude and variable amplitude tests using a replicating technique. At predetermined cycles, testing was stopped at a tensile peak causing maximum opening of any cracks which had developed. After removing the extensometer and cleaning the specimen, methyl acetone was injected between the specimen and a strip of acetyl cellulose film 0.034 mm thick. The softened cellulose film was wrapped around the specimen and allowed to dry creating a permanent impression of the specimen surface. Each surface replica covered approximately 60% of the specimen surface within the gage section. Two replicas were taken each time the test was stopped, each 180° apart, so that crack growth over the entire gage section was recorded. The extensometer was reinstalled and fatigue cycling continued.

By taking replicas at approximately every 10% of expected life, the crack growth could be recorded throughout the test. With the use of an optical microscope, crack length from the replicas could be measured with a resolution of $\pm$ 0.01 mm.

VOLUMETRIC CRACK GROWTH

After failing in fatigue, some samples were sectioned longitudinally (parallel to the axis of stress). These sections were polished using standard metalographic techniques. Final polishing was done with 0.05 micron alumina powder. Specimens were inspected under an optical microscope to determine if any fatigue cracks had initiated at graphite flakes in the interior of the specimen.

IV. RESULTS AND DISCUSSION

CRACK GROWTH

Strain-life data from the constant amplitude fatigue tests is given in Table 3 and shown graphically in Figure 5. Evaluation of the surface replicas taken throughout the tests show that cracks initiate very early during the fatigue life of a specimen. Fatigue cracks were always noticed to have initiated at the tips of graphite flakes with surfaces normal to the direction of loading. The crack then propagated through the matrix material toward another graphite flake. The process of fatigue crack growth is one of linking many graphite flakes and linking multiple crack systems; the net directon of propagation being normal to the direction of loading. During each test, the first surface replica was taken after about 10% of the fatigue life had been exhausted. In all the specimens evaluated, some fatigue crack growth could be observed from the first replica. In some cases, the crack which ultimately propagated to failure had not begun to grow when the first replica was taken but initiated a short time later.

On any single specimen, multiple cracks were initiated. The number of cracks which did initiate, however, was still very small compared with the number of graphite flakes visible on the specimen surface. Fash [3] noted that as strain amplitude increased the number of crack systems initiated also increased. Many of the cracks, after initiation, would halt as they reached adjacent graphite flakes or as the tensile load decreased. If two or more cracks had developed at the same cross-section, they would often link together and form a dominant crack. After one crack had reached a length of 3 mm, through a combination of crack growth and crack linking, its growth dominated to failure. After one crack reached this length, the peak tensile load decreased rapidly halting the propagation of other cracks. In most samples, only the failure crack was found to be greater than 3 mm in length at the completion of cycling. The majority of the specimen life, 80-90%, was spent growing the dominant fatigue crack to a length of about 3 mm; after this, crack length increased very quickly to failure. Figure 6 shows crack growth over the life of the specimens. In Figure 7, crack length is plotted verses normalized life (a vs. N/N_f). Normalized life is defined as cycles completed/cycles to failure.

TENSILE LOAD DROP

Associated with the development of fatigue cracks is a decline in the peak tensile load. As seen in Figure 8, peak tensile load drops continuously over the duration of the test. Fash [3] noted that this tensile load drop is closely related to the formation of fatigue cracks and is not the result of cyclic softening. The peak tensile load vs.normalized life curve (Figure 8) has two regions. The first region includes most of the life of a specimen and shows a gradual decline in peak tensile load. The second region includes the final 5-10% of fatigue cycling and shows a rapid decrease in the peak tensile load. During the first 80-90% of life, the peak tensile load decreases almost linearly to a magnitude of 80-90% of the peak load at the initiation of fatigue cycling. Over this interval, the dominant fatigue crack has grown to a length of about 3 mm. Samples cycled at a larger strain amplitude show a slightly larger rate of percent tensile load drop in this region. During the last 5% of fatigue life the tensile load decreases very rapidly. Approximately 70% of the load carrying ability of the specimen in lost in this interval. Fash [3] found that tensile load drop data was dependent on the location of the fatigue crack relative to the extensometer. If the failure crack develops between the contact points of the extensometer, much less load is required to reach the control strain than if the failure crack had developed on the side of the specimen opposite the extensometer. This variation in load becomes more significant as the crack size increases.

HYSTERESIS LOOPS AND MEAN STRESS EFFECTS

Socie and Fash [1] found that a parameter of the form ($\sigma_{max} * \Delta\varepsilon / 2$) provides a single relationship for both strain control and stress control fatigue tests as well as accounting for mean stress effects. They found a power law

$$\sigma_{max} * \Delta\varepsilon/2 = 1.82\ (2N_f)^{-0.25}\ \text{MPa} \qquad (1)$$

to give a good fit for all the test data collected for a pearlitic gray iron. As seen in Figure 9, the above equation fits the constant amplitude test data for the pearlitic gray iron tested in this study as well.

Fatigue cycling at the second of the two strain amplitudes was begun after a compressive reversal of the first amplitude. A slight tensile stress was required to return the specimen to zero strain after the compressive reversal. Starting fatigue cycling st the second strain amplitude with a slight tensile stress increased the value of σ_{max} recorded compared to the value of σ_{max} that would be expected for a constant amplitude test of the same amplitude. In the most severe situation ($\Delta\varepsilon_1/2=.002$, $\Delta\varepsilon_2/2=.001$), the value of σ_{max} was increased by about 10%. If equation 1 is used to estimate the effect of this increase in σ_{max}, the predicted reversals to failure is reduced by 32%. Starting fatigue cycling with a slight tensile stress seems to have had litte effect on the life of a specimen.

Hysteresis loops recorded for one of the six variable amplitude tests are shown in Figure 10. The first recorded hysteresis loop at the second strain amplitude is superimposed on the last recorded loop at the first strain amplitude.

DAMAGE CALCULATIONS

Miner's linear damage rule suggests using N/N_f as a single state variable to measure fatigue damage in a material.

$$D = \Sigma\, N_i \;/\; N_{fi} \qquad (2)$$

Where N_i = the number of cycles at amplitude i, N_{fi} = the number of cycles to failure at amplitude i, D = a scalar damage parameter; damage is predicted to occur when D=1. Miner's rule assumes that damage is accumulated linearly over the life of a specimen and that the rate of damage accumulation is independent of $\Delta\varepsilon$ and σ_0. Socie, Fash and Leckie [6] found that a continuum damage model gives better life estimates than Miner's rule for cast iron subject to variable strain histories. This model proposes that the rate of damage accumulation is a function of the current state of damage, the mean stress, and the strain amplitude.

$$\dot{D} = f\ (D,\ \Delta\varepsilon/2,\ \sigma_0) \qquad (3)$$

Downing [8] has investigated a number of physically measurable quantities that may be used to assess the state of damage in cast irons; these are crack length, stress drop (in strain control tests), hysteresis energy drop, and unloading modulus drop. For pearlitic gray iron, all of these quantities yield roughly the same results when used in the continuum damage model.

In practice, crack length is an important method for assesing damage in a component. If crack length is used as a measure of damage, the continuum damage model asserts that equivalent crack lengths represent equal states of damage regardless of the load history which produced the crack.

For the six variable amplitude strain histories evaluated in this testing program, the continuum damage model predicts lives similar to those predicted by Miner's rule. This result is expected because the crack length vs. normalized life curves, a vs. N/N_f, are nearly coincident for the three strain levels tested (see Figure 7). Thus if a single horizontal (constant crack length) line representing a constant damage state was passed through all three a vs. N/N_f curves, the horizontal line would intersect all three curves at nearly the same value of N/N_f.

For a given constant strain amplitude, the fatigue lives between samples could easily vary by a factor of four or more. When fatigue damage is estimated based on N/N_f, an average value of N_f is used. If extreme values of N_f are used, significant differences in fatigue damage will be calculated. Because the fatigue lives among samples tested at a specific strain amplitude vary, the crack length vs. life curves also vary. By normalizing the life for each test, N/N_f, the a vs. N/N_f curves for one strain amplitude are nearly coincident. By measuring the crack length at a known number of cycles and using these curves, it may be possible to accurately predict the number of cycles remaining to failure. Therefore for constant amplitude testing, crack length is a better measure of the state of damage of cast iron than N/N_f.

The damage accumulated at the first of the two strain amplitudes was estimated using two methods. First, damage was calculated by dividing the cycles completed at that strain amplitude by the number of cycles to failure that would be expected in a constant amplitude test (Miner's rule).

$$D_1 = N_1 / N_{f1} \quad (4)$$

Second, by using the a vs. N/N_f curves previously discussed and the crack length, a, developed during cycling at the first amplitude a value of normalized life, N/N_f, can be estimated.

$$D_1^* = N / N_f \quad (5)$$

The damage done at the second strain amplitude was computed using Miner's rule.

$$D_2 = N_2 / N_{f2} \quad (6)$$

This value was added to the estimated damage from the first strain amplitude to give the computed damage at failure for the specimen.

$$D = D_1 + D_2 \quad \text{or} \quad D = D_1^* + D_2 \quad (7)\ (8)$$

A damage model which works perfectly should give the damage at failure equal to unity for any strain history.

Using tensile load drop data to estimate the state of damage was more difficult. During the first 80% of life, the tensile load drops continuously, but at a very small rate, so that slight changes in the measured load would predict very different lives. The location of the fatigue cracks relative to the extensometer changed for each specimen causing slightly different load drop rates for a given strain amplitude. Removing and reinstalling the extensometer 8-10 times during a test introduces some error. Slight changes in the point of zero strain can lead to changes in the peak tensile stress. The test control software collected data at every power of two cycle so that at longer lives, the interval between data collection points was large. Tensile load drop data, if measured carefully, may be useful in predicting the state of damage of cast irons.

VARIABLE AMPLITUDE TEST RESULTS

Results from the variable amplitude fatigue tests may be found in Table 4. When the first strain amplitude was smaller than the second, the Lo-Hi case, the experimental life was close to that predicted by Miner's rule. The computed damage at failure ($D = D_1 + D_2$) ranged from 0.65 to 1.25 for these tests compared to the ideal value of one. By using the crack length and the a vs. N/N_f curve to obtain a value of normalized life at the first strain amplitude, slightly better life predictions resulted. The computed damage at failure ($D = D_1^* + D_2$) ranged from 0.85 to 1.05. Crack length vs. life for a typical Lo-Hi test may be found in Figure 11.

For tests where the first strain amplitude was larger than the second strain amplitude, Hi-Lo, the experimental life consistently exceeded the life predicted by Miner's rule. The damage at failure for these tests ranged from 1.05 to 4.75. By using crack length to normalize the life at the first strain amplitude, variation in experimental life over predicted life was larger. The computed damage at failure ranged from 1.15 to 4.75;

in four of the six Hi-Lo tests, the computed damage at failure was between 1.15 and 1.5. If the damage at the first strain amplitude is normalized based on crack length, the damage at failure calculated for Lo-Hi tests was always approximately one while the damage at failure calculated for Hi-Lo tests was always greater than one.

The most significant increase in experimental life over predicted life occurred when a specimen was first cycled at a strain amplitude of .0015 followed by cycling at a strain amplitude of .001. Using this strain history, the number of cycles to failure at the second strain amplitude was 156000 which is about five times the life to failure predicted by Miner's rule(30000) and seven times the predicted life to failure if the damage at the first strain amplitude was normalized based on crack length(21000). The damage at failure for this specimen calculated by Miner's rule was 3.0 and was 3.25 if normalized life is used. A second specimen tested with this history showed similar results.

Evaluation of the surface replicas for this strain history show that at the second strain amplitude of $\Delta\varepsilon/2$ = .001, the crack growth was never completely arrested, but was much slower than the constant amplitude crack growth over its entire life. See Figure 12. At a crack length of 1mm, for example, constant amplitude cycling at $\Delta\varepsilon/2$ = .001 shows a crack growth rate of 1.3×10^{-4} mm/cycle. A specimen cycled first at $\Delta\varepsilon/2$ = .0015 until the crack reached a length of 0.75 mm then cycled at $\Delta\varepsilon/2$ = .001 until failure shows a crack growth rate at 1 mm of only

1.4×10^{-5} mm/cycle. Similar reductions in the crack growth rate occur over the entire life of the specimen.

These results from the variable amplitude testing indicate that normalizing the life based on crack length at the first strain amplitude will lead to better life predictions for Lo-Hi tests. When the strain history is Hi-Lo, there appears to be some load interaction effect. The load interaction effect may be similar to the crack growth retardation observed in wrought materials after single or multiple stress overload cycles. The state of damage in cast irons, therefore, cannot be completely described with a single state theory. Damage appears to be a function not only of crack length but also of some residual stress state in the material.

$$D = f\ (a, \sigma_{res}) \qquad (9)$$

Applying Miner's rule, a continuum damage model or normalizing the life based on crack length can be used and should lead to conservative life estimates.

VOLUMETRIC CRACK GROWTH

Two samples, after they had failed in fatigue, were sectioned longitudinally, polished and examined under an optical microscope. Small fatigue cracks had initiated at some of the graphite flake tips inside the specimen and were propagating toward the surface. All of these cracks were small, the largest observed being about 0.3 mm in length. See Figure 13.

V. CONCLUSIONS AND RECOMMENDATIONS

Fatigue cracks initiate very early during the life of the pearlitic gray cast iron tested. Fatigue life is determined by a complex process of crack growth and crack linking, so that a crack propagation based damage model will be more useful in predicting fatigue life than a crack initiation model.

Crack length data is useful in predicting the life remaining to failure for constant amplitude fatigue tests. Crack length data may also be used to estimate the damage done during the first block of a Hi-Lo or Lo-Hi test. By measuring the crack length after the first block of fatigue cycling is complete the crack length vs. normalized life curves developed from constant amplitude testing may be used to calculate a value of normalized life for this block. Using normalized life as a measure of damage done at the first strain amplitude in a Lo-Hi test leads to a better life prediction than if Miner's rule is applied alone. When the strain history was Hi-Lo, the experimental life consistently exceeded the life predicted by Miner's rule. If normalized life is used to estimate damage done at the first strain amplitude in a Hi-Lo test, the experimental life again exceeded the predicted life

Experiments indicate that a Lo-Hi strain sequence is more damaging than a Hi-Lo strain sequence indicating that load interaction effects may be significant. To understand better the effects of load interaction, more constant amplitude and variable amplitude testing should be done to provide a better statistical base from which to make conclusions. A conservative estimate of service life for variable amplitude tests can be computed by applying Miner's rule or a continuum damage model. If further testing shows that there is a significant load interaction effect in alternating between different strain amplitudes, it may be useful to investigate the application of principals from LEFM crack growth models to cast iron.

A damage theory using crack length as a single state measure of fatigue damage is not accurate. Some information about the past load history which caused the crack to grow to the measured length must be known to assess damage. Crack length, however, can still be used to make a quick estimate of the state of damage in a component.

Changes in mean stress can have a large influence on the fatigue life of gray cast iron. For the six step histories tested, the mean stress at the second strain amplitude varied little from the mean stress that would be expected for constant amplitude testing at the same amplitude. This slight change in mean stress probably had little effect on fatigue life.

Fatigue cracks which initiate and grow through the interior of the specimen have been observed. These cracks were small and their effect on fatigue life has not been determined.

TABLE 1. MATERIAL CHEMISTRY
PEARLITIC GRAY IRON

C	Si	Mn	S	P	Ti	Ni	Cr	Mo	Cu
3.30	2.20	.44	.02	.01	.01	.06	.03	.01	.40

TABLE 2. MECHANICAL PROPERTIES

Modulus of Elasticity, E (Tension/Compression)	84/108 GPa
Yield Strength .2%	185 MPa
Ultimate Strength	228 MPa
True Fracture Ductility	0.0122
Bulk Hardness	180 BHN
Eutectic Cell Size	0.14 mm
ASTM A247 Flake Designation	60% Type A, 40% Type D, Size 4

TABLE 3. CONSTANT AMPLITUDE TEST RESULTS

Specimen	$\Delta\varepsilon / 2$	N_f
23	.001	47100
24	.002	1780
32	.0015	9300
33	.0015	4930
35	.0015	3390
41	.0015	14000
42	.001	72700
43	.002	2340

This data is shown graphically in Figure 5.

TABLE 4. VARIABLE AMPLITUDE TEST RESULTS

SPECIMEN	STRAIN AMPLITUDE FIRST / SECOND	CYCLES COMPLETE STRAIN 1	CYCLES TO FAILURE STRAIN 2	DAMAGE AT STRAIN 1 D(a)*	DAMAGE AT STRAIN 1 N/N_{f1}**	CALCULATED DAMAGE AT FAILURE*** D(a)	CALCULATED DAMAGE AT FAILURE*** N/N
25	.001 / .002	25000	1170	.35	.40	.90	.95
26	.002 / .001	1050	70000	.30	.50	1.50	1.70
28	.002 / .001	1050	38000	.60	.50	1.20	1.10
30	.001 / .002	40000	530	.80	.65	1.05	.90
31	.001 / .001	25000	6600	.20	.40	1.05	1.25
34	.0015/ .001	4000	263200	.55	.55	4.75	4.75
36	.0015/ .002	4100	396	.70	.55	.90	.75
37	.002 / .0015	1050	3300	.70	.50	1.25	1.05
38	.0015/ .002	3000	530	.60	.40	.85	.65
39	.002 / .0015	750	5170	.45	.35	1.15	1.05
40	.0015/ .001	3000	156700	.65	.40	3.25	3.00

* D(a), Damage normalized based on crack length

** N/N_f , Damage calculated by Miner's Rule

*** Damage at second strain amplitude cal-ulated by Miner's Rule

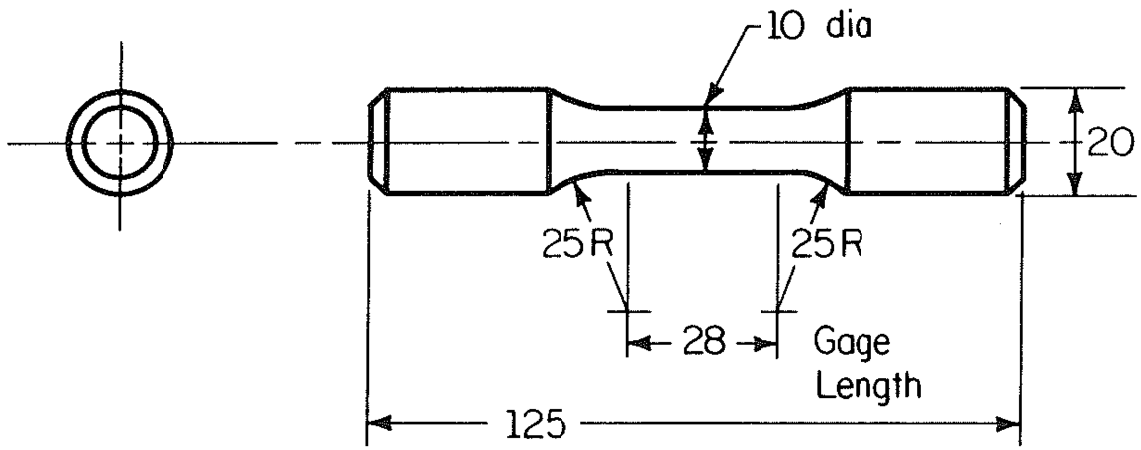

Figure 1. Test Specimen Geometry - Dimensions In mm

.1 mm

.1 mm

2% Nital

Figure 2. Flake Form and Matrix Microstructure

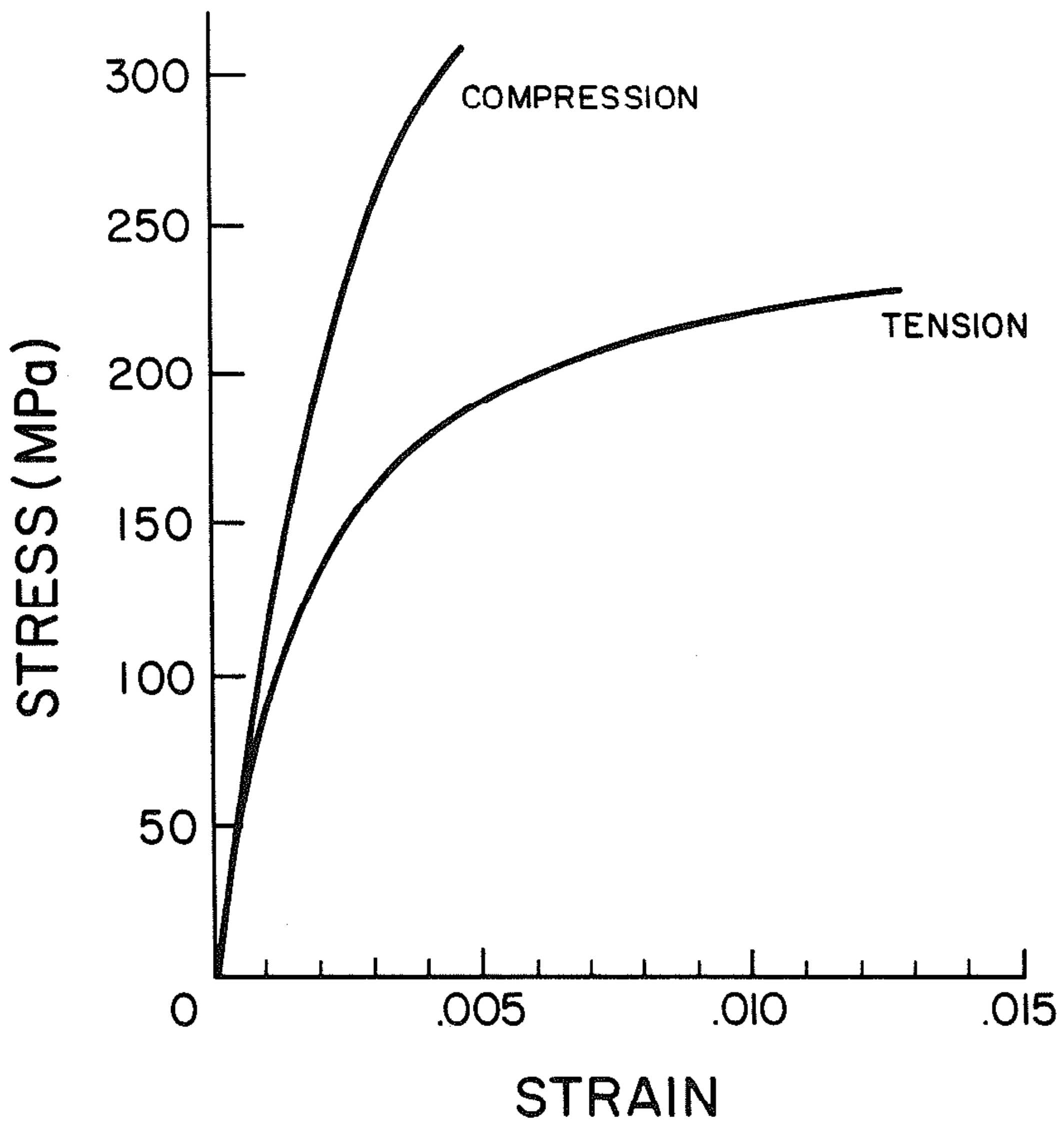

Figure 3. Monotonic Stress-Strain Response

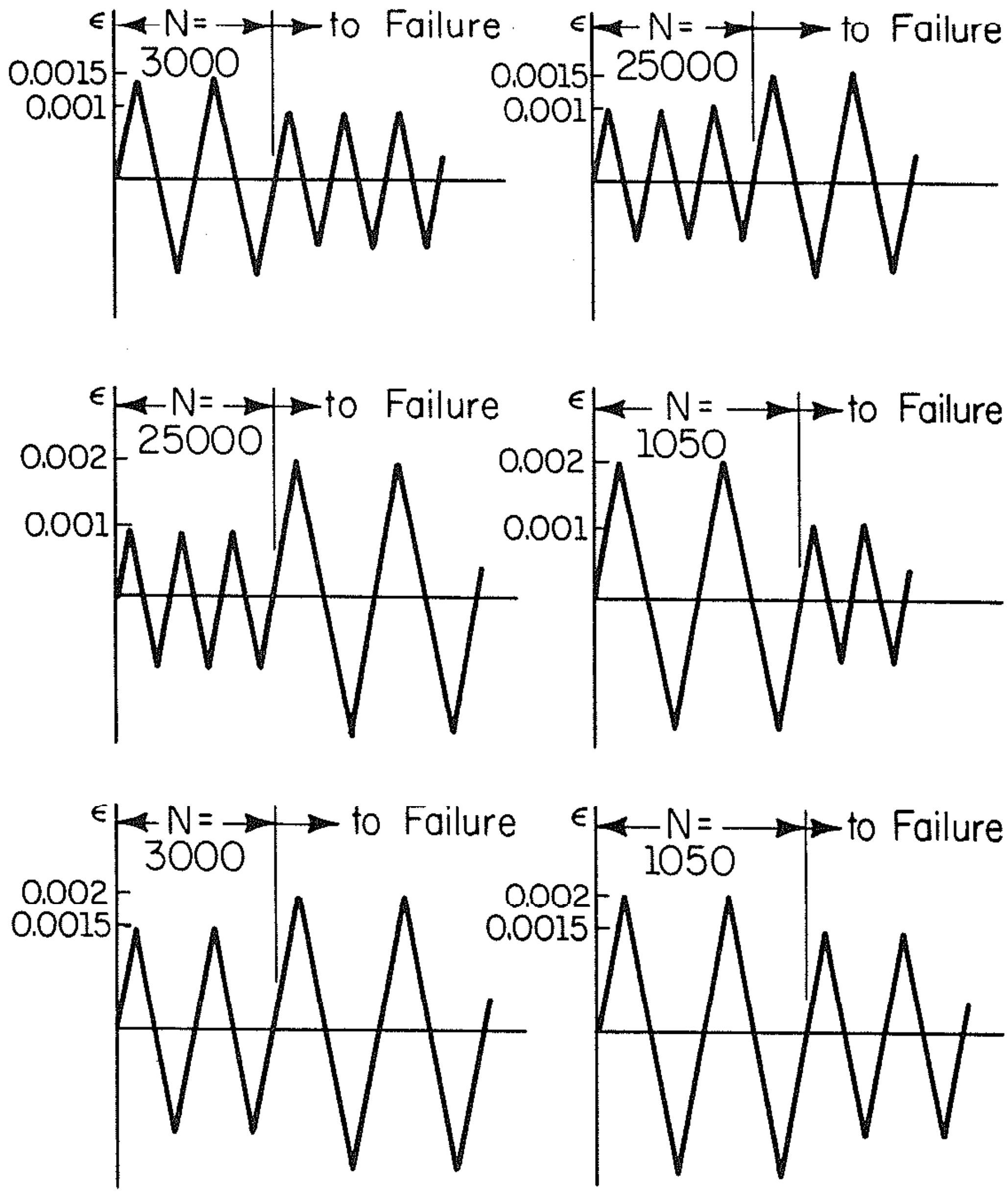

Figure 4. Strain histories

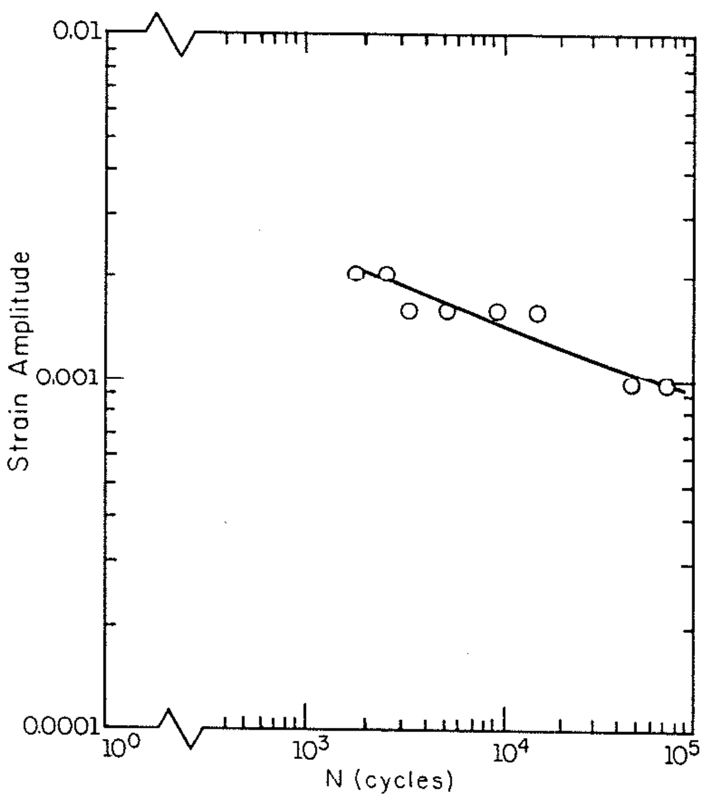

Figure 5. Strain - Life Curve

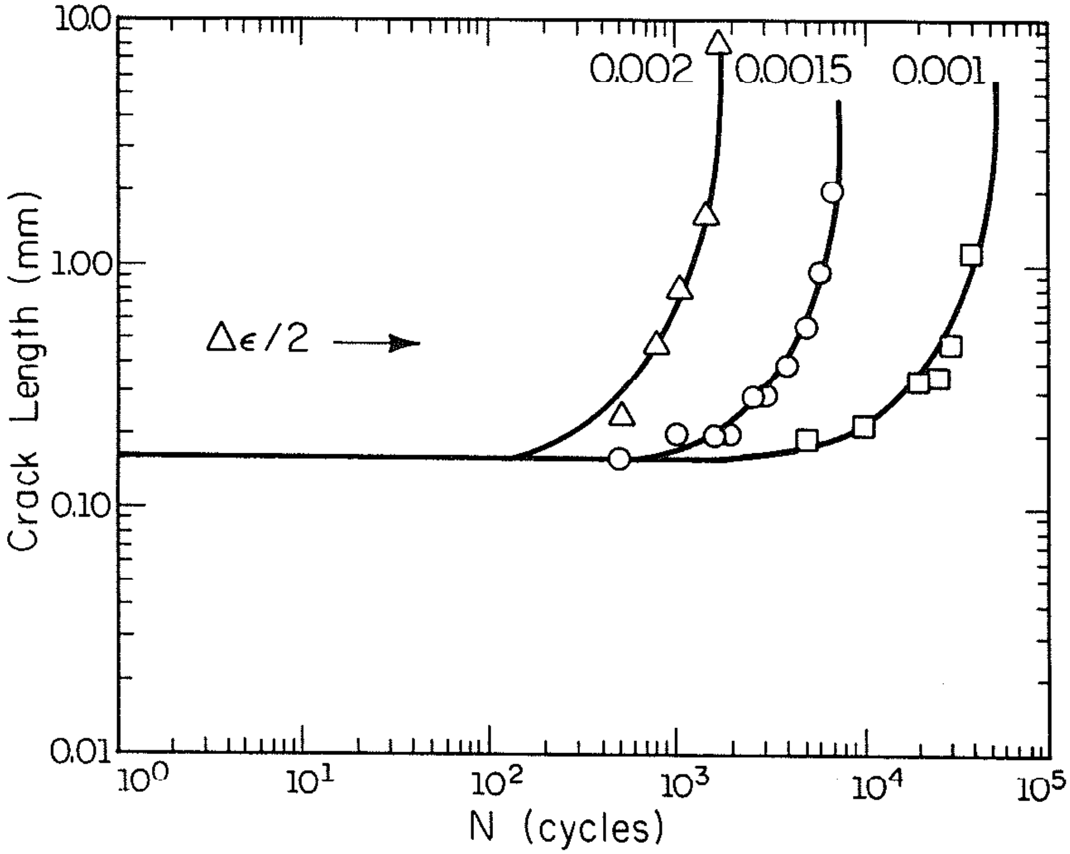

Figure 6. Crack Growth vs. Applied Cycles

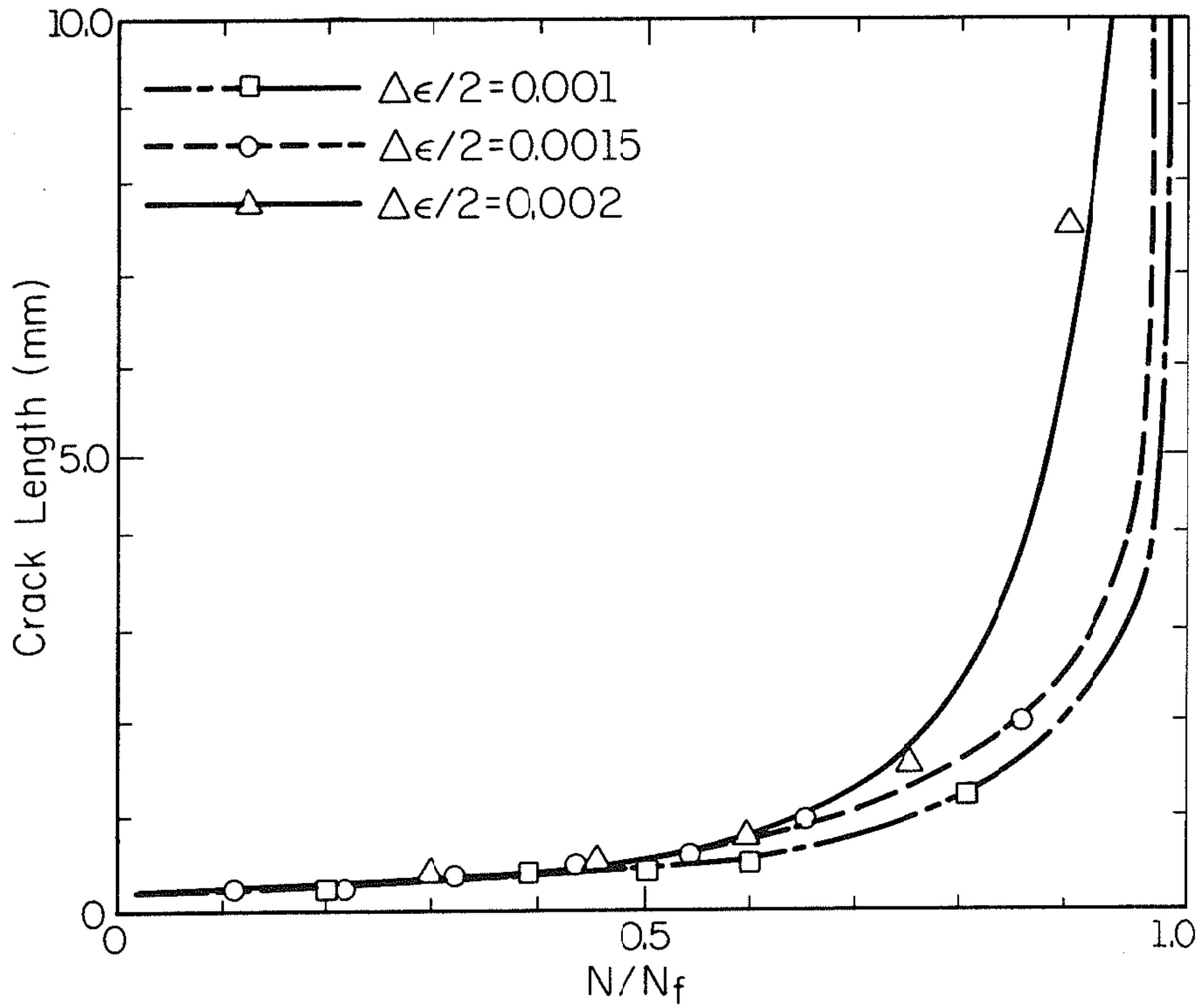

Figure 7. Crack Length vs. Normalized Life, a vs. N/N_f

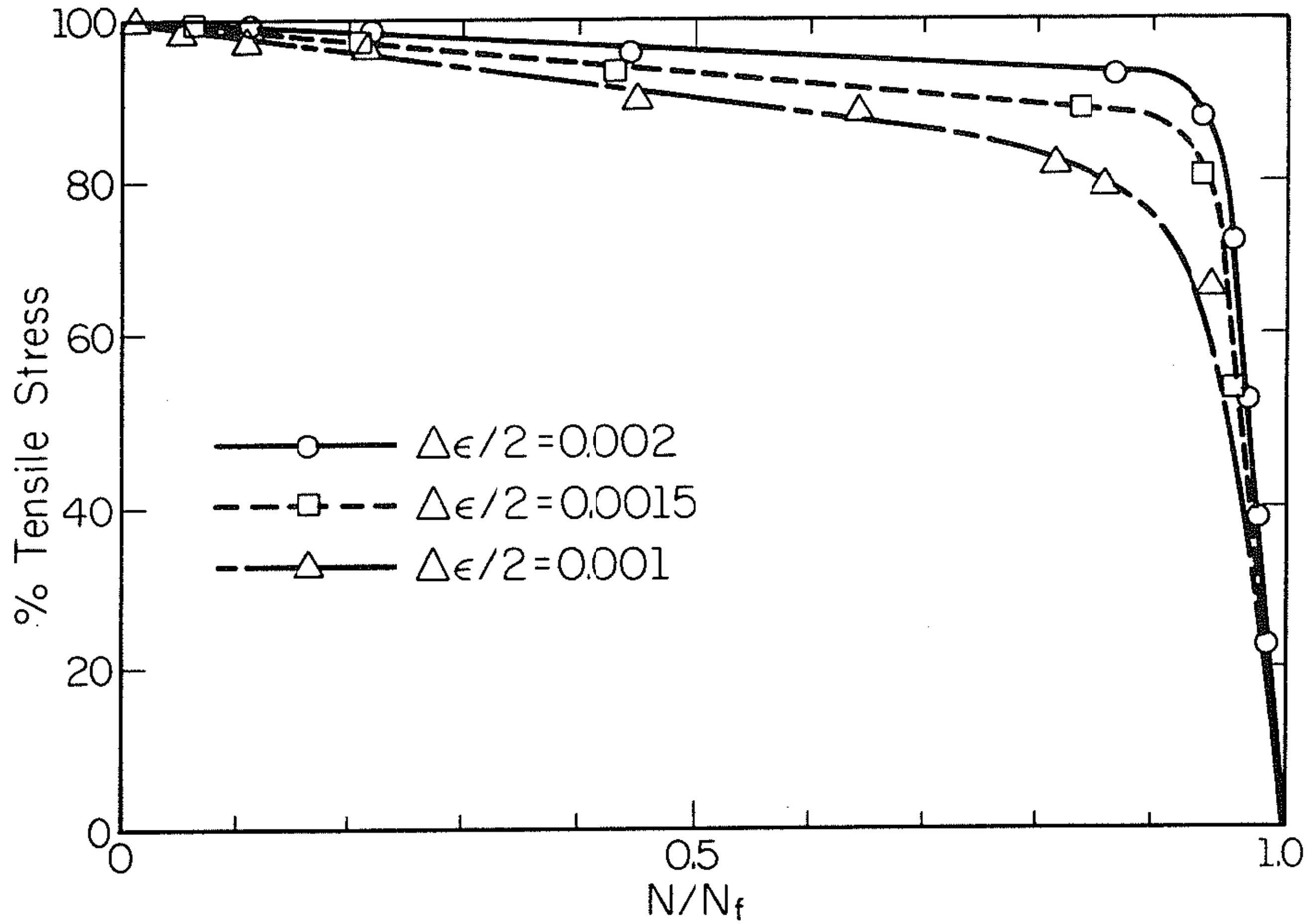

Figure 8. Tensile Load Drop vs. N/N_f

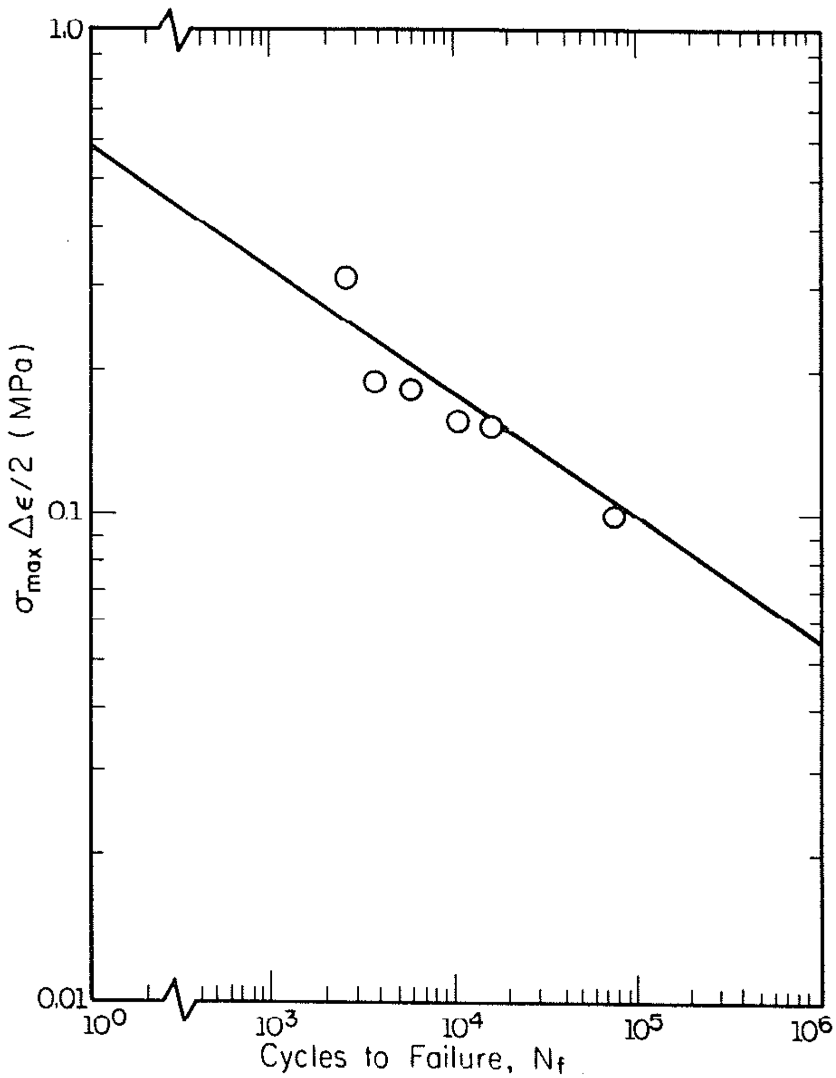

Figure 9. Constant Amplitude Fatigue Test Results

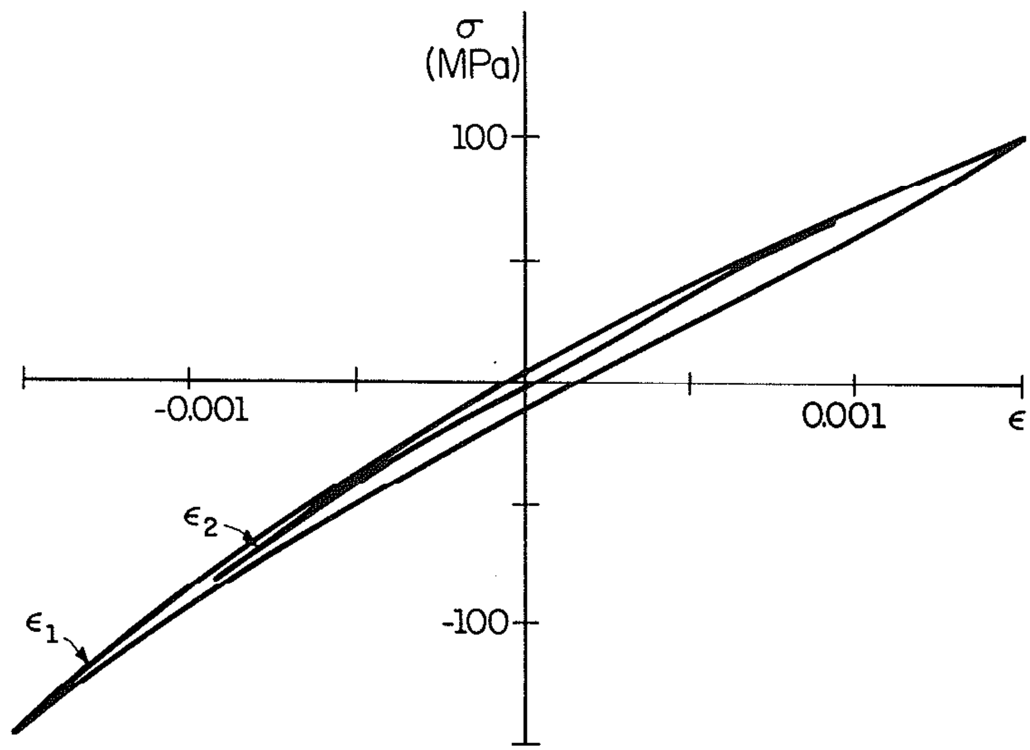

Figure 10. Hysteresis Loops $\frac{\Delta\varepsilon_1}{2}$ = .0015, (at cycle N_1 = 2098)

$\frac{\Delta\varepsilon_2}{2}$ = .001, (at cycle N_2 = 1)

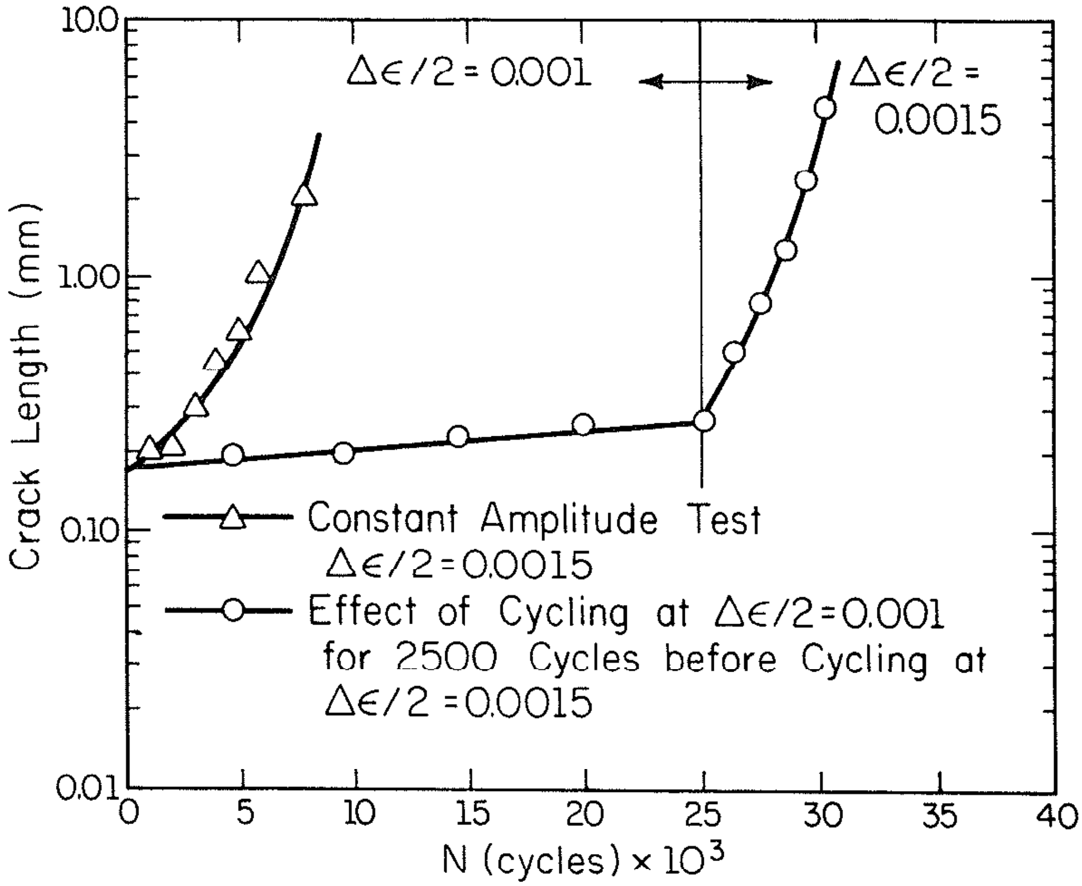

Figure 11. Crack Growth vs. Life Lo-Hi Test

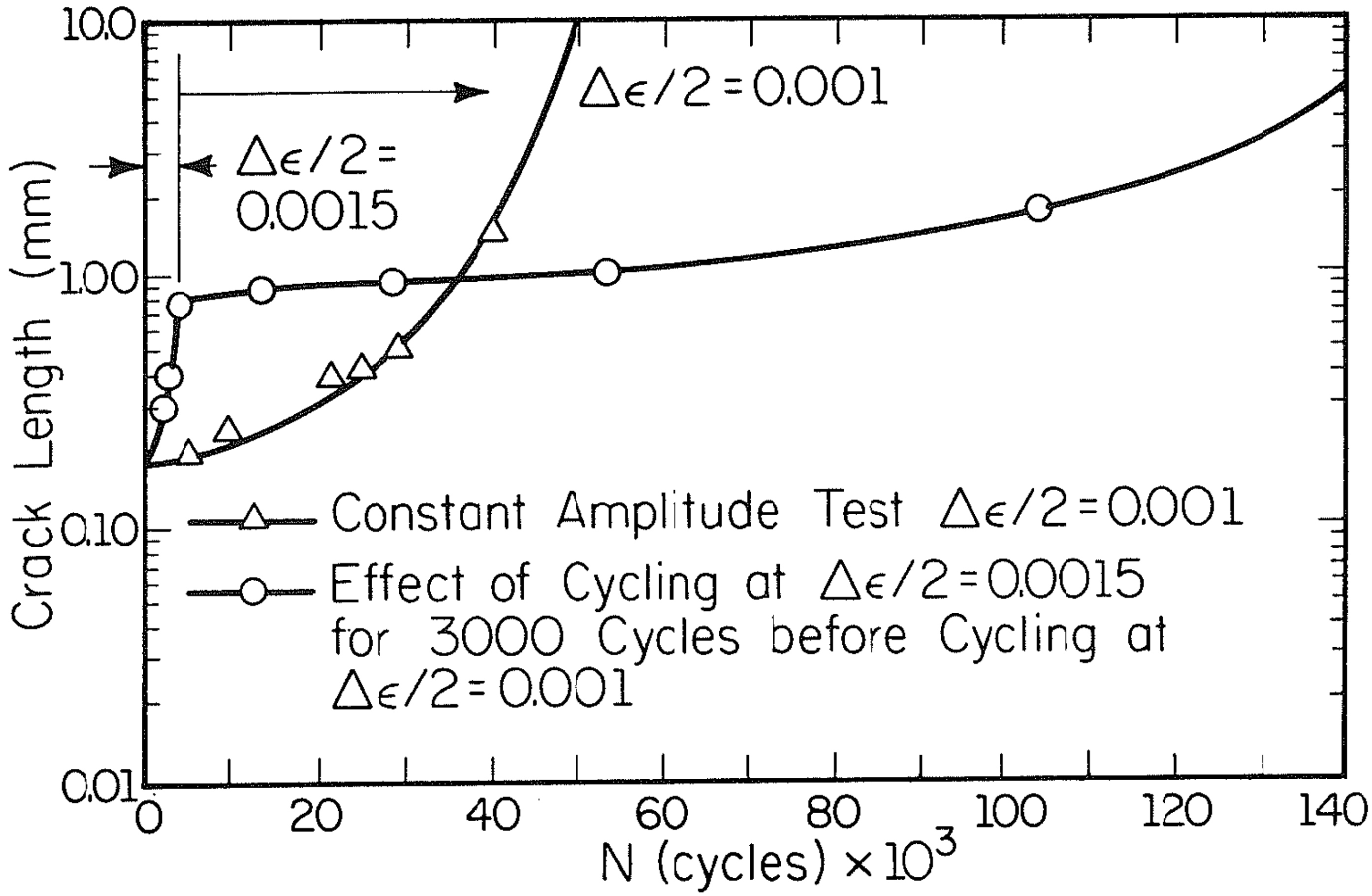

Figure 12. Crack Growth vs. Life Hi-Lo Test

0.05 mm

Figure 13. Fatigue Crack Initiation in the Interior of the Specimen

REFERENCES

1. Socie, D.F., Fash, J.W. , and Downing, S.D. , "Fatigue of Gray Iron," Fracture Control Program, Report No.44 College of Engineering, University of Illinois at Urbana-Champaing, October 1982.

2. Fuchs, H.O. and Stephens, R.I., "Metal Fatigue in Engineering," Wiley-Interscience, New York, 1980.

3. Fash, J.W., "Fatigue Crack Initiation and Growth in Gray Cast Iron," Fracture Control Program, Report No. 35, College of Engineering, University of Illinois at Urbana-Champaign, October 1980.

4. Hua, C., "Fatigue Crack Growth in Nodular Cast Iron," Fracture Control Program, Report No. 47, College of Engineering, University of Illinois at Urbana-Champaign, February 1983.

5. Mitchell, M.R., "Effects of Graphite Morphology, Matrix Hardness, and Structure on the Fatigue Resistance of Gray Cast Iron," Society of Automotive Engineers, Inc., Report No. 750198 (1975).

6. Socie, D.F., Fash, J.W. and Leckie, F.A., "A Continuum Damage Model for Fatigue Analysis of Cast Iron," ASME Conference on "Advances in Life Prediction Methods," September 1983.

7. "Methods of Evaluating the Microstructure of Graphite in Iron Castings," ASTM Designation:A247, Plate I (Graphite Form Types), Plate II (Graphite Flake Type Chart), and Plate III (Graphite Size), American Society for Testing and Materials, 1916 Race Street, Philadelphia, Pa 19103.

8. Downing, S.D., "Modeling Cyclic Deformation and Fatigue Behavior of Cast Iron Under Uniaxial Loading," Materials Engineering-Mechanical Behavior, Report No. 101, College of Engineering, University of Illinois at Urbana - Champaign, January 1984.